Gépészet 2008
Budapest, 29-30.May 2008.

G-2008-J-04

EXPERIMENT-BASED CRITERION FOR THE CRACK STABILITY ANALYSIS IN COMPOSITE MATERIALS

András Szekrényes
Assistant Professor, Department of Applied Mechanics, Budapest University of Technology and Economics
H-1521 Budapest, PoB 11, Hungary, Phone: +36 1 463 1170, Fax: +36 1 463 3471, e-mail: szeki@mm.bme.hu

Abstract: *The traditional criterion of the crack stability in fracture mechanics states that the stability of the crack propagation is determined by the derivative of the energy release rate with respect to the crack length. This work proposes a new experiment-based criterion for the crack stability analysis of fracture mechanical systems. A large number of experiments performed shows that the stability of the crack propagation depends on the derivative of the critical displacement with respect to the crack length. Thus, a new criterion is developed and compared to the traditional one. It is shown that in each case the two criteria lead to approximately the same restriction considering the stable zone of crack propagation.*

Keywords: *interlaminar fracture, crack stability, split cantilever-beam, energy release rate*

1. INTRODUCTION

The crack stability problem is an important issue in the interlaminar fracture tests. For a certain fracture mechanical configuration it is worth the effort to predict what we could expect during the measurements: stable or unstable crack propagation. In the literature a very large amount of experimental work has been published including mode-I [1,2], mode-II [3,4] and mixed-mode I/II [5,6] configurations. Except for some of them (which mainly investigate the stability of mode-II configurations) each ignores the problem of crack stability. For instance, in the mode-I double-cantilever beam (DCB) specimen the crack propagation is always stable. On the other hand under mode-II the stability problem can limit the length of the initial crack, while under mixed-mode I/II (being the combination of the mode-I and mode-II) the instability problem can also take place.

The traditional stability criterion [7] states that the stability depends on the derivative of the energy release rate (ERR) with respect to the crack length: if it is zero or negative then stable crack propagation can be expected. Otherwise instability may take place. Based on this criterion the limit value of the crack length can be determined for a system of which geometrical and material parameters are known. For the common mode-II beam-like specimens the limit of the crack length is known. On the contrary, the relevant literature does not contain any information for mixed-mode I/II and II/III cases, where the problem of instability also arises.

In this paper a novel stability criterion is developed, which is essentially an experiment-based one. To formulate the new criterion a large number of tests were performed on unidirectional E-glass/polyester composite including mode-I, mode-II, mixed-mode I/II and II/III tests. For each test the traditional and the novel criteria were applied and their restrictions to the crack length are compared. In each case the agreement seemed to be very good. Apart from some minor differences the new method leads essentially to the same restrictions as the traditional criterion

2. THE TRADITIONAL CRITERION

In accordance with the linear elastic fracture mechanics the definition of the crack driving force in a linear elastic body with including a crack is [7]:

$$G_C = \frac{dW}{dA} - \frac{dU}{dA}, \tag{1}$$

where W is the work of external forces, U is the strain energy of the system and A is the area of crack face, Eq. 1 is called the critical ERR. It is convenient to use the Irwin-Kies expression to determine the ERR in delaminated slender beams [7]:

$$G_C = \frac{P^2}{2b}\frac{dC}{da}, \tag{2}$$

where C is the compliance and P is the applied load required for crack propagation. The crack stability of the system is determined by the derivative of the ERR with respect to the crack length. If dG_C/da is zero or negative then stable crack propagation may be expected:

$$\frac{dG_C}{da} \le 0. \tag{3}$$

Eq. 3 can be considered under the fixed load or fixed grip conditions [8]. We consider the latter one as a more realistic condition. Eq. 2 can be transformed as ($C=\delta/P$):

$$G_C = \frac{\delta^2}{2bC^2}\frac{dC}{da}, \tag{4}$$

where δ is the displacement of the specimen at the point of load application. The derivative of the ERR with respect to the crack length is [8]:

$$\frac{dG_C}{da} = \frac{\delta^2}{2bC^2}\left[\frac{d^2C}{da^2} - \frac{2}{C}\left(\frac{dC}{da}\right)^2\right]. \tag{5}$$

It is seen that the stability analysis requires the determination of the compliance vs. crack length relationship. The $C(a)$ curve could be determined in three ways: analytically, numerically or/and experimentally. The analytical solutions are available only for those systems, which can be considered as beams and plates. The numerical solution requires more work, especially when a three-dimensional model is necessary. Finally, the most work is required for the experiments (specimen manufacturing, preparation, experiments, data reduction, scatter of the data etc.). In the following some well-known fracture mechanical tests are utilized for the stability analysis. The analysis includes the mode-I double-cantilever beam (DCB) [1], the mode-II end-notched flexure (ENF) [8], four point bend end-notched flexure (4ENF) [4], end-loaded split (ELS) [1,2], over-notched flexure (ONF) [9], the mixed-mode I/II single-cantilever beam (SCB) [10], single-leg bending (SLB) [10], over-leg bending (OLB) [10] (Fig.1) and the mixed-mode II/III modified split-cantilever beam (MSCB) [11] specimens (Fig. 2). In previous publications the compliance of these configurations has been calculated based on linear beam theories [10, 12].

2.1 SOME COMMON SPECIMEN TYPES

In accordance with Eq. 5 it is necessary to express the compliance of the system. The following notations are used in Figs. 1 and 2: a (crack length), b (specimen width), L and $2L$ (span length), E_{11} (flexural modulus), E_{33} (through thickness modulus), G_{13}, G_{23} (shear moduli in the x-z and y-z plane), ν_{13} (Poisson's ratio), k=5/6 (shear correction factor), c (uncracked length in the ONF and OLB specimens) and s (the position of applied load). Referring to Fig. 1a the compliance of the mode-I DCB specimen is [10]:

$$C^{DCB} = \frac{8a^3}{2bh^3E_{11}} + \frac{2a^3}{bh^3E_{11}}\left[f_{W1} + \frac{f_{SV}}{2} + \frac{1}{k}\left(\frac{h}{a}\right)^2\left(\frac{E_{11}}{G_{13}}\right)\right]. \tag{6}$$

Fig. 1 b-c-d and e schematically represents the mode-II ENF, 4ENF, ELS and ONF specimens. The compliances of these systems are [9,10]:

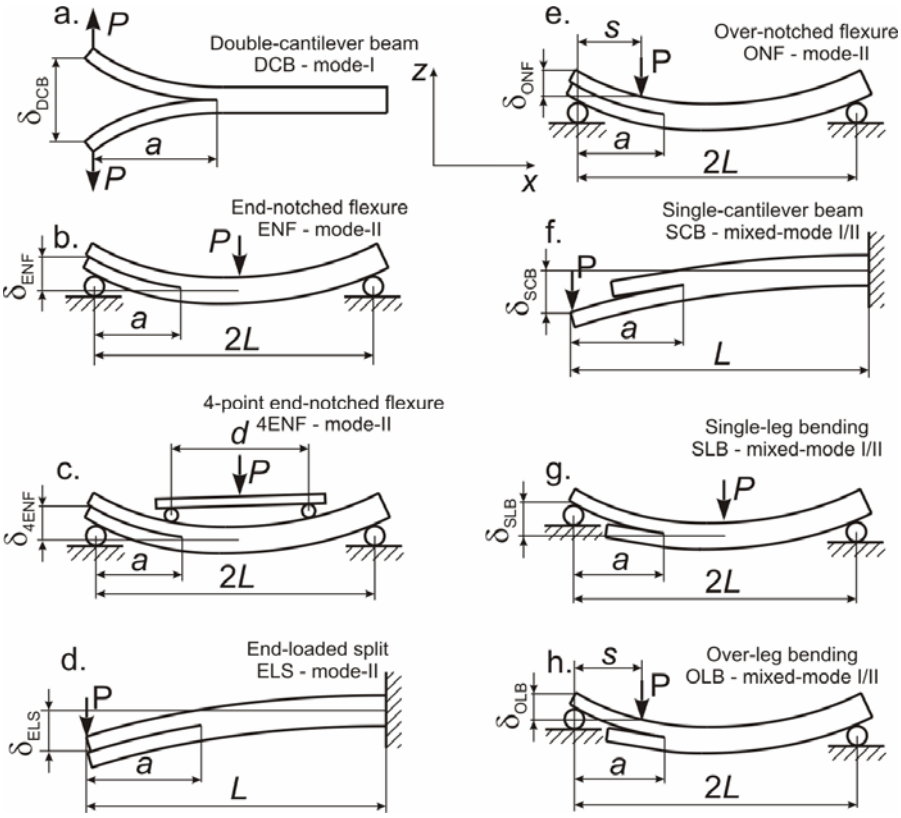

Fig. 1. *Schematic illustration of the DCB, ENF, 4ENF, ELS, ONF, SCB, SLB and OLB composite specimens*

$$C^{ENF} = \frac{3a^3 + 2L^3}{8bh^3E_{11}} + \frac{2L}{8bhkG_{13}} + \frac{a^3}{8bh^3E_{11}} f_{SH1}, \tag{7}$$

$$C^{4ENF} = \frac{(9a + 6L - 12s)s^2}{8bh^3E_{11}}, \tag{8}$$

$$C^{ELS} = \frac{3a^3 + L^3}{2bh^3E_{11}} + \frac{L}{2bhkG_{13}} + \frac{a^3}{2bh^3E_{11}} f_{SH1} + \frac{3}{\pi}\frac{L^2}{2bh^2E_{11}}\left(\frac{E_{11}}{G_{13}}\right)^{\frac{1}{2}}, \tag{9}$$

$$C^{ONF} = \frac{s^2c^3}{8bh^3E_{11}L^2}[1 + 4\frac{a}{c} + 8\frac{aL}{c^2} + 16\frac{aL^2}{c^3} + 8\frac{Ls(s-4L)}{c^3}] + \frac{s(2L-s)}{8bhkG_{13}L} + \frac{s^2c^3}{8bh^3E_{11}L^2} f^*_{SH1}. \tag{10}$$

In the sequel three mixed-mode I/II configurations are utilized, all of them produce an approximately constant mixed-mode ratio of G_I/G_{II}=1.33. Following the order of Fig. 1 (f, g and h), the compliance of the SCB, SLB and the OLB specimens become:

$$C^{SCB} = \frac{7a^3 + L^3}{2bh^3E_{11}} + \frac{a + L}{2bhkG_{13}} + \frac{a^3}{2bh^3E_{11}}[f_{W1} + f_{SH1} + \frac{f_{SV}}{2}] + \frac{3}{\pi}\frac{L^2}{2bh^2E_{11}}\left(\frac{E_{11}}{G_{13}}\right)^{\frac{1}{2}}, \tag{11}$$

$$C^{SLB} = \frac{7a^3 + 2L^3}{8bh^3E_{11}} + \frac{a + 2L}{8bhkG_{13}} + \frac{a^3}{8bh^3E_{11}}[f_{W1} + f_{SH1} + \frac{f_{SV}}{2}], \tag{12}$$

$$C^{OLB} = \frac{s^2 c^3}{8bh^3 E_{11} L^2}[1 + 8\frac{a}{c} + 16\frac{aL}{c^2} + 32\frac{aL^2}{c^3} + 16\frac{Ls(s-4L)}{c^3}] + \frac{s[4L(2L-s)-sc]}{8bhkG_{13}L^2} + \\ + \frac{s^2 c^3}{8bh^3 E_{11} L^2}[f_{W1}^* + f_{SH1}^* + \frac{f_{SV}^*}{2}], \tag{13}$$

where the factors are:

$$f_{W1} = 5.07\left(\frac{h}{a}\right)\left(\frac{E_{11}}{E_{33}}\right)^{\frac{1}{4}} + 8.58\left(\frac{h}{a}\right)^2\left(\frac{E_{11}}{E_{33}}\right)^{\frac{1}{2}} + 2.08\left(\frac{h}{a}\right)^3\left(\frac{E_{11}}{E_{33}}\right)^{\frac{3}{4}}, \tag{14}$$

$$f_{SH1} = 0.98\left(\frac{h}{a}\right)\left(\frac{E_{11}}{G_{13}}\right)^{\frac{1}{2}} + 0.43\left(\frac{h}{a}\right)^2\left(\frac{E_{11}}{G_{13}}\right),\ f_{SV} = \frac{12}{\pi}\left(\frac{h}{a}\right)\left(\frac{E_{11}}{G_{13}}\right)^{\frac{1}{2}}, \tag{15}$$

furthermore in the ONF and OLB specimens (Eqs. 10 and 13) the factors, f_{W1}^*, f_{SV}^* and f_{SH1}^* are:

$$f_{W1}^* = f_{W1}\big|_{a=c},\ f_{SV}^* = f_{SV}\big|_{a=c},\ f_{SH1}^* = f_{SH1}\big|_{a=c}. \tag{16}$$

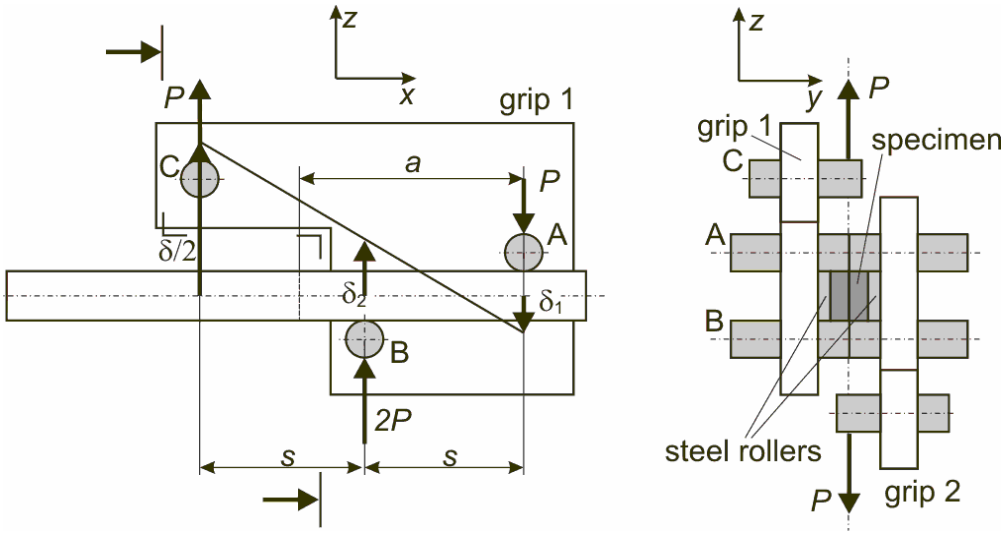

Fig. 2. *Schematic illustration of the MSCB specimen*

Finally the compliance of the mixed-mode-II/III MSCB specimen is in Fig. 2 is:

$$C = \frac{8a^3}{b^3 h E_{11}}[f_{EB1} + f_{TIM1} + f_{FT1} + f_{S-V1} + f_{CT1}], \tag{17}$$

where:

$$f_{EB1} = 1 - 6\left(\frac{s}{a}\right) + 12\left(\frac{s}{a}\right)^2 - 6\left(\frac{s}{a}\right)^3,\ f_{TIM1} = 0.3\left(\frac{b}{a}\right)^2\left(\frac{E_{11}}{G_{13}}\right),\ f_{FT1} = 0.19\frac{1}{\varsigma}\left(\frac{b}{a}\right)^2\left(\frac{E_{11}}{G_{12}}\right), \tag{18}$$

$$\mu = \left(\frac{G_{13}}{G_{12}}\right)^{\frac{1}{2}},\ \varsigma = 1 - 0.63\mu\frac{h}{b},\ f_{SV1} = [0.48 - 1.91\left(\frac{s}{a}\right) + 1.91\left(\frac{s}{a}\right)^2]\left(\frac{b}{a}\right)\left(\frac{E_{11}}{G_{13}}\right)^{\frac{1}{2}}, \tag{19}$$

$$f_{CT1} = 0.75\left(\frac{b}{a}\right)^3 E_{11}(\lambda + \lambda_{ST})(1 + \ln\frac{h^3}{(\lambda + \lambda_{ST})PR}),\ \lambda = \frac{1 - \nu_{13}^2}{E_{33}},\ \lambda_{ST} = \frac{1 - \nu_{ST}^2}{E_{ST}}, \tag{20}$$

where E_{ST} and ν_{ST} are the elastic properties of the steel rollers A and B in Fig. 2.

2.2. APPLICATION OF THE TRADITIONAL CRITERION

Substituting the above given compliances into Eq. 5 the stability of the system can be represented as a function of the normalized crack length. The solution of Eq. 5 for the specimens demonstrated in Fig. 1 is depicted in Fig. 3a-c. Namely, Fig. 3a plots the results of the DCB, ELS and SCB specimens. The reason for this classification is that these coupons are

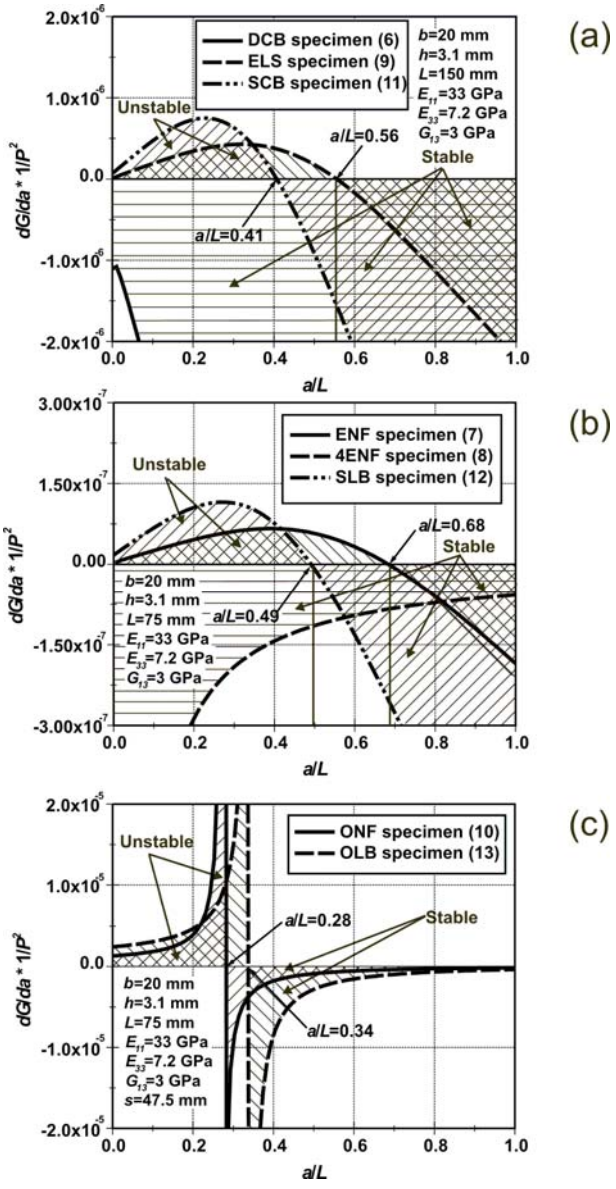

Fig. 3. *Crack stability of the DCB, ELS, SCB (a), ENF, 4ENF, SLB (b), and ONF, OLB (c) specimens in accordance with the traditional criterion.*

loaded at the end, they can be investigated in the same crack length range and finally, the specimens testify very similar behavior. Running through the results it is seen that there is no stability problem in the DCB specimen, while the restrictions in the ELS and SCB specimens are: $a \leq 0.56L$ and $a \leq 0.41L$, respectively.

In Fig. 3b the results for the ENF, 4ENF and the SLB systems are classified. Similarly to Fig. 3a, these systems can be investigated in the same crack length range. The 4ENF test

promotes always stable crack propagation (it has been highlighted by others [4]), on the other hand the chosen crack length of the ENF and SLB specimens must satisfy the requirements of $a \leq 0.68L$ and $a \leq 0.49L$, respectively. Finally, the stability chart of the ONF and OLB specimens are shown in Fig. 3c. Although mathematically there is a restriction for both cases, physically "*a*" should always be higher than "*s*" (the position of the applied load from the left specimen end, refer to Fig. 1e and h), which – under the present geometrical parameters (s=47.5 mm, L=75 mm) – involves that $a \leq 0.63L$ for both systems, i.e. it states a strongest restriction than those in Fig. 3c.

The stability chart of the MSCB specimen is shown in Fig. 4 including four different values of "*s*". It is seen that the when s=26 mm then the stable ranges are $a \geq 74.3$ mm and $a \leq 48.3$ mm, i.e. if a_0=150 mm, then: $a/a_0 \geq 0.49$ and $a/a_0 \leq 0.32$ for stable crack propagation in the MSCB specimen.

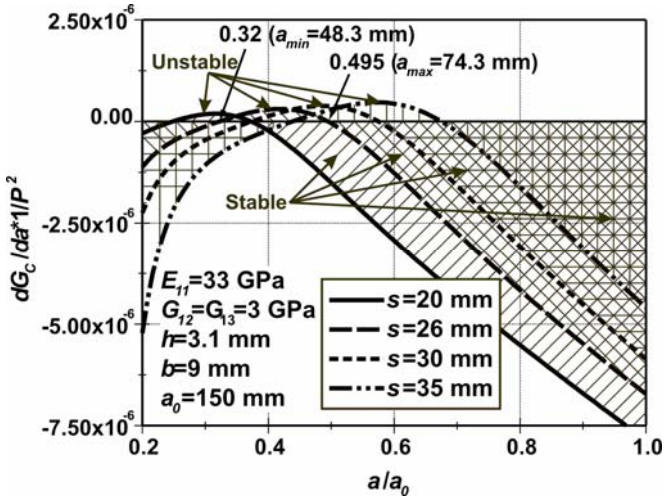

Fig. 4. *Crack stability of the MSCB specimen in accordance with the traditional criterion.*

As a summary of the results it seems that the application of this criterion is quite simple. However, when there is no analytical solution, then the $C(a)$ function should be determined by experimental measurements and then a proper curve-fit technique is necessary. The relevant method is called as compliance calibration (CC) [1,2,3,4,6], which is the most accurate data reduction technique in fracture toughness measurements. The drawback of the method is that its accuracy depends upon the number of points used for the curve-fit process. Further complications take place if the compliance of the system is relatively small, leading to the large scatter of the measured data. It should be mentioned that although in this case the compliance vs. crack length relationship may be obtained by finite element calculations, it requires the precise determination of the material properties (elastic moduli and Poisson's ratios) of the material. This issue is relatively simple when the bending dominates the deformation; however when the shape of the specimen strongly differs from a slender beam, then shearing, transverse deformation and Poisson's effect may contribute significantly to the deformation process. The additional material properties (G_{12}, G_{13}, G_{23}, ν_{12}, ν_{13}, ν_{23}, E_{22} and E_{33}) can be approximated by rule of mixtures, or – utilizing different tests – experimental measurements. In such cases due to the large number of measurement and specimen types required for testing it is worth the effort to take the novel criterion presented below into consideration.

3. THE NOVEL CRITERION

The mentioned drawbacks of the traditional criterion motivated the author to develop another one, which can be applied also in those cases, where the traditional one seems to be failed, i.e.: when the compliance of the system is relatively small, and we do not know the material properties with sufficient accuracy. In what follows the novel criterion is established. It is important to note that the novel criterion is essentially an experiment-based approach. Therefore, a large amount of experiments were performed on the configurations, shown in Figs. 1-2.

3.1 EXPERIMENTAL WORK

Specimen preparation

The constituent materials of present E-glass/polyester composite were procured from Novia Ltd. The properties of the E-glass fiber are E=70 GPa and ν=0.27, while for the unsaturated polyester resin are E=3.5 GPa and ν=0.35. Both were considered to be isotropic. The unidirectional ($[0°]_{14}$) E-glass/polyester specimens with nominal thickness of $2h$=6.2 mm, width of b=20 mm (except for the MSCB specimen where b=9 mm was applied), and fiber-volume fraction of V_f=43% were manufactured in a special pressure tool. A polyamide (PA) insert with thickness of 0.03 mm was placed at the midplane of the specimens to make an artificial starting defect. A significant advantage of the present E-glass/polyester material is the transparency, which allows of the visual observation of crack initiation/propagation. The tool was left at room temperature until the specimens became dry. Then the specimens were removed from the tool and were further left at room temperature until 4-6 hours. At the final stage the specimens were cut to the desired length and were precracked in opening mode of 4-5 mm by using a sharp blade. The reason for that was in this case it was possible to make a straight crack front, which is important in the case of the crack length measurement and the observation of the crack initiation.

Material properties, specimen dimensions

The flexural modulus was determined from a three-point bending test with span length of $2L$=150 mm using six uncracked specimens with $2h$=6.2 mm and b=20 mm. The experiments resulted in E_{11}=33 GPa. The additional properties were predicted from simple rules of mixture, in this way E_{33}=7.2 GPa, G_{13}= G_{23}=3 GPa and ν_{13}=0.27 were obtained.

Crack initiation tests

In all the presented cases the fracture behavior of the systems were investigated in quite extended crack length ranges. The specimen dimensions were $2h$=6.2 mm, b=20 mm, and the whole length of the specimens was 180 mm. At each crack length a unique specimen was used and was loaded up to fracture initiation. The applied load was measured by using an Amsler testing machine, while the displacement of the specimen was recorded by a mechanical dial gauge. In the following the performed test types are detailed.

In the DCB test (Fig. 1a) steel hinges were bonded to the specimen faces. The DCB specimens with the following crack lengths were prepared: a=25, 30, 35, 40, 45, 50, 55, 60, 65, 70, 75, 80, 90, 100, 110, 120, 130, 140 and 150 mm.

For the ENF test (Fig. 1b) eleven specimens were used to test the material in the range of a=25 to 75 mm with 5 mm increments. The specimens were put into a three-point bending setup, the method of the load and displacement measurement was the same as that of the DCB specimen. The span length was $2L$=150 mm.

In the case of the 4ENF (Fig. 1c) coupon the investigated crack length range was: a=45 to 105 mm with 5 mm increments. The specimens were loaded through a steel block,

which divided the applied load into two equal parts inducing pure bending in the central region of the specimen. Load and displacement recordings were also performed. The span length was 2*L*=150 mm.

The mode-II ELS (Fig. 1d) test was performed using specimens with *a*=35, 40, 45, 50, 55, 60, 65, 70, 75, 75, 80, 90, 100, 110, 120, 130 and 140 mm. The coupons were put into a clamping fixture and were loaded at the end. The distance from the load application and the clamped end was *L*=150 mm. The load and displacement was recorded until crack initiation.

For the ONF (Fig. 1e) test the range of *a*=50 to 105 mm with 5 mm increments was covered. The specimens were loaded excentrically to the vertical centerline of the system, the distance from the left specimen side was *s*=47.5 mm, the span length was 2*L*=150 mm.

The mixed-mode I/II SLB (Fig. 1f) test was performed in the range *a*=20 to 75 mm with 5 mm increments under the same geometrical parameters as the ENF test.

The investigated crack length range in the SCB specimen (Fig. 1g) was: *a*=20, 25, 30, 35, 40, 45, 50, 55, 60, 65, 70, 75, 75, 80, 90, 100, 110, 120, 130 and 140 mm under the same conditions as the ELS specimen.

The OLB specimens (Fig. 1h) including crack lengths in the range of *a*=50 to 115 mm with 5 mm increments were prepared. The geometry of the system corresponded to those of the ONF test.

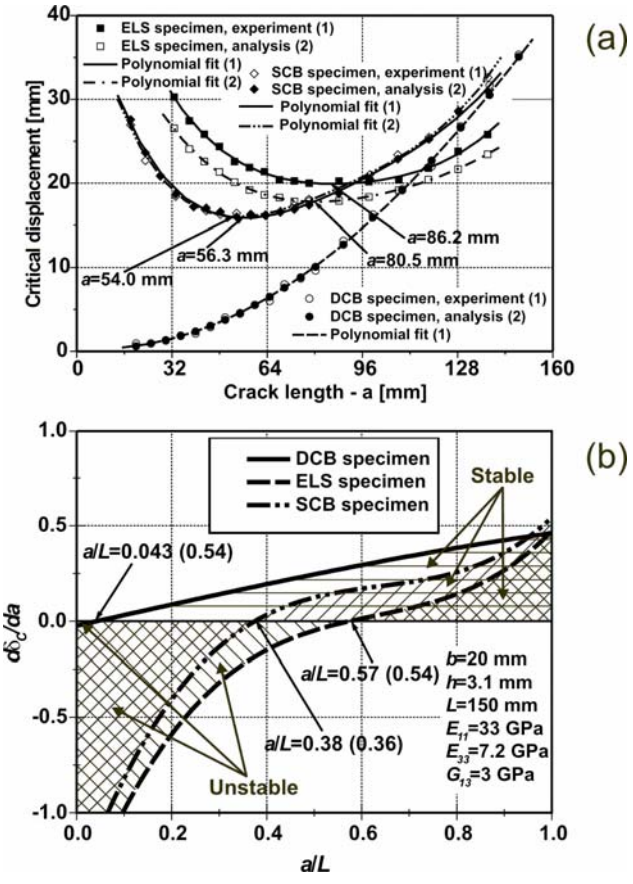

Fig. 5. *The experimentally measured critical displacements (a) and the crack stability chart of the DCB, ELS and SCB specimens (b)*

Finally, the MSCB system (Fig. 2) 13x4 specimens were used with the following crack lengths: *a*=45, 50, 55, 60, 65, 70, 75, 80, 85, 90, 95, 100 and 105 mm, at each crack length four specimens were tested.

3.2. RESULTS

The most important conclusion of this part is based on an experimental observation. In some of the investigated systems it was observed that it was not possible to investigate the crack propagation if the crack length of interest was lower then a certain value, i.e. the stability of the system was restricted by the crack length and the geometrical parameters of the system. In all the investigated cases if instability was observed then the fact of the instability was represented by a sudden crack jump (in some cases the jump was 50-60 mm from the initial crack tip), which prevented the measurement of the crack length and load values. The point of instability (if instability took place) was always at that point, where the critical displacement reached its minimum value. Based on a large number of experiments performed on E-glass/polyester composite specimens the novel criterion can be formulated as:

$$\frac{d\delta_C(a)}{da} \geq 0, \tag{21}$$

i.e. the stability of crack propagation is determined by the derivative of the critical displacement with respect to the crack length. The critical displacement is denoted as the value of the specimen displacement at the point of crack initiation. In the case of the DCB specimen the critical displacement is equivalent to the crack opening displacement (COD) [7], however in all of the other cases there is no relationship between the COD and the critical displacement since the COD theorem is essentially related to mode-I problems.

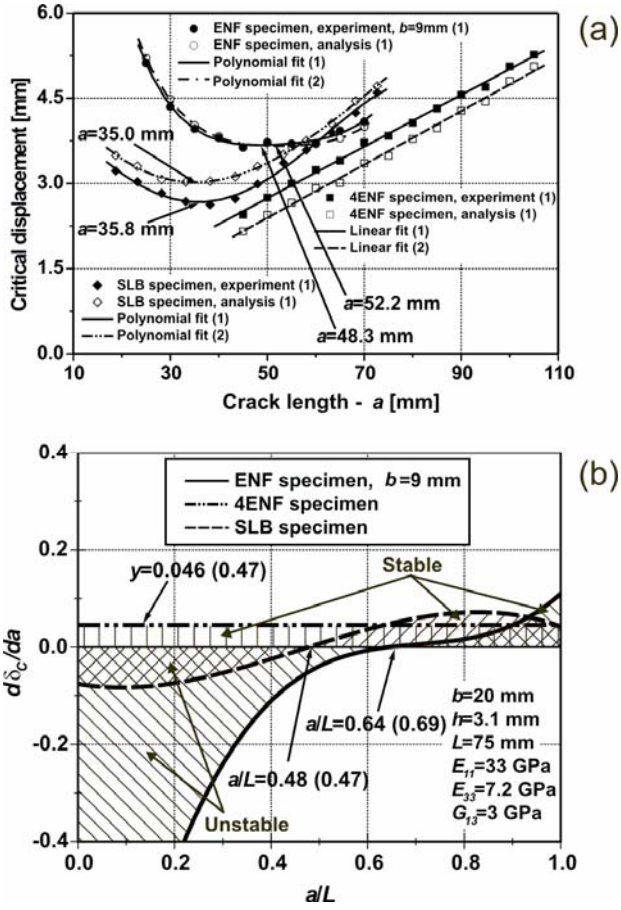

Fig. 6. *The experimentally measured critical displacements (a) and the crack stability chart of the ENF, 4ENF and SLB specimens (b)*

Fig. 5a represents the measured critical displacement values measured from the DCB, ELS and SCB tests as the function of the crack length. The measured displacement values were fitted by a second, third or fourth order polynomial as the function of the crack length and the point where the derivative of the curve was horizontal was believed to be the limit value regarding the stability of the system. Even the analytical solution is given in Fig. 5a indicating a very good agreement with the experimentally measured point. Fig. 5b shows the crack stability chart calculated by using Eq. (21), where the limit ratios (a/L) are also highlighted. The values in the parentheses were obtained from the analytical solutions. In a similar fashion Figs. 6a-b plot the same results for the ENF, 4ENF and SLB configurations. The only difference is that in the case of the 4ENF a linear fit was made. For the ONF and OLB specimens the experimental results and the stability diagrams are demonstrated in Figs. 7a-b. Finally Fig. 8 shows the critical displacements as the function of the crack length in the MSCB specimen, the fitted curve and the crack length, where the derivative of the fitted curve is zero.

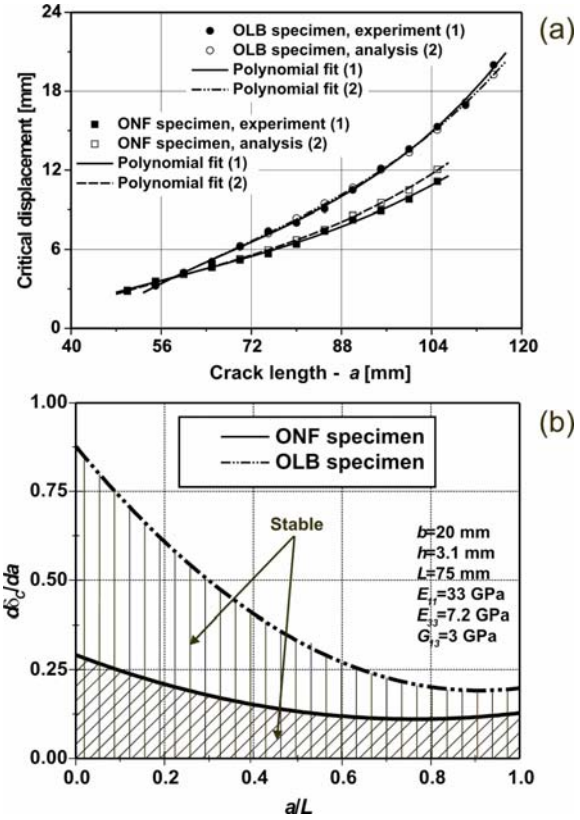

Fig. 7. *The experimentally measured critical displacements (a) and the crack stability chart of the ONF and OLB specimens (b)*

4. COMPARISON

Considering the results of the traditional and the novel criterion the following conclusions may be drawn. In those cases, where instability takes place the two criteria agrees excellently, this can be justified by the limit values of a/L. The traditional criterion shows that for the ELS and SCB specimens the limit is a/L=0.56 and a/L=0.41 (Fig. 3a), respectively while the novel criterion states that a/L=0.57 and a/L=0.38 (Fig. 5b), for the same systems, respectively. The difference is -1.8% in the former and +7.3% in the latter case. Both criteria indicate stable crack propagation for the DCB specimen. For the ENF and SLB test the same results are: a/L=0.68 and a/L=0.64 (+6%), a/L=0.49 and a/L=0.48 (+2%), respectively. The

crack propagation is always stable in the 4ENF specimen, as it is confirmed by both criteria. For the ONF and OLB specimen there are no stability problems in accordance with both criteria. Finally for the MSCB specimen the analysis provides an unstable range between $48.3 \leq a \leq 72.3$, while the novel criterion indicates only a transition at a=72.46 mm. It involves an extremely small difference compared to the upper limit of the unstable zone.

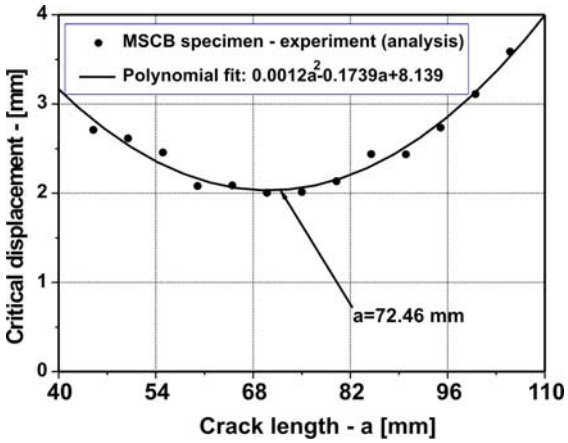

Fig. 8. *The experimentally measured critical displacements of the MSCB specimen*

So it seems that the novel criterion shows an excellent agreement with the traditional one in all the presented cases (except in the MSCB specimen, where it does not predict the lower range of the unstable zone). Therefore it may be assumed that the agreement would be similar in other type of fracture mechanical configurations.

In the following the advantages and drawbacks of the novel criterion over the traditional one are highlighted. First of all the traditional criterion requires the determination of the compliance-crack length relation, either analytically, numerically or experimentally. The first method can be applied only if the system behaves as a slender beam, or it is a plate. The numerical and analytical calculation requires the accurate determination of the material properties. This is especially difficult if the tested material is strongly anisotropic. As regarding to the experimental compliance measurement it is a possible case that the compliance of the system is relatively small, which can lead to significant deviation of the data and serious errors in the curve-fit process and the derivative of the compliance curve, and so the limit value of the ratio a/L would be determined erroneously.

In contrast, being an experiment-based one the novel criterion does not require the determination of the material properties. However the relatively small compliance (displacement) values can give misleading results. It should be mentioned that for the identification of the limit ratio of stability is possible even in those cases where the experimental error is relatively huge, because displaying the measured critical displacement values as the function of the crack length it is possible to identify approximately the minimum value (which theoretically corresponds to the limit of stability). It is important to note that in this case it is not recommended to fit the points and to plot the charts, because the curve fit process leads to further smoothing and distortion of the results.

5. CONCLUSIONS

In this work a novel crack stability criterion was established. Several fracture mechanical systems including mode-I, mode-II, mixed-mode I/II, and mixed-mode II/III

configurations were tested experimentally and based on an observation it was found that the stability of the system depends on the derivative of the critical displacement (displacement at crack initiation) of the specimens at the point of load application.

The results obtained were compared to those by the traditional criterion of crack stability. The two criteria agreed very well considering the limit ratios (a/L) of the stability, and corresponded even in those cases when there was no stability problem. All these results confirmed the accuracy and applicability of the novel criterion. It is a reasonable assumption that the novel criterion is applicable to other types of materials and even to different fracture mechanical systems. It has been highlighted that in some cases the novel criterion is more reasonable to apply – for example when the material is anisotropic or the compliance of the system is difficult to measure precisely – than the traditional one.

ACKNOWLEDGEMENTS

This research work was sponsored by the Hungarian National Research Fund (OTKA) under Grant No. 34040.

REFERENCES

[1] Hashemi S, Kinloch J, Williams JG. The effects of geometry, rate and temperature on mode I, mode II and mixed-mode I/II interlaminar fracture toughness of carbon fibre/poly(ether-ether ketone) composites. Journal of Composite Materials 1990;24:918-956.

[2] Hashemi S, Kinloch J, Williams JG. Mechanics and mechanisms of delamination in a poly(ether sulphone)-fibre composite. Composites Science and Technology 1990;37:429-462.

[3] Schön J, Nyman T, Blom A, Ansell H. Numerical and experimental investigation of a composite ENF-specimen. Engineering Fracture Mechanics 2000;65:405-433.

[4] Schuecker C, Davidson B. Evaluation of the accuracy of the four-point bend end-notched flexure test for mode II delamination toughness determination. Composites Science and Technology 2000;60:2137-2146.

[5] Crews Jr JH, Reeder JR. A mixed-mode bending apparatus for delamination testing. NASA Technical Memorandum 100662, 1988, August, 1-37.

[6] Reeder JR, Crews Jr JH. Mixed-mode bending method for delamination testing. AIAA Journal 1990;28:1270-1276.

[7] Anderson TL. Fracture Mechanics – Fundamentals and Applications. Third Edition. Boca Raton, London, New York, Singapore: CRC Press, Taylor & Francis Group 2005.

[8] Carlsson LA, Gillespie JW, Pipes RB. On the analysis and design of the end notched flexure (ENF) specimen for mode II testing. Journal of Composite Materials 1986;20:594-604.

[9] Szekrényes A. Mode-II fracture in E-glass-polyester composite. Journal of Composite Materials 2005,39(19):1747-1768.

[10] Szekrényes A. Improved analysis of unidirectional composite delamination specimens. Mechanics of Materials 2007;39:953-974.

[11] Sharif F., Kortschot M.T., Martin R.H. Mode III Delamination Using a Split Cantilever Beam. In: Composite Materials: Fatigue and Fracture – Fifth Volume ASTM STP 1230, Ed.: Martin R.H., ASTM, Philadelphia 1995. p. 85-99.

[12] Szekrényes A. Delamination fracture analysis in the G_{II}-G_{III} plane using prestressed transparent composite beams. International Journal of Solids and Structures 2006;44:3359-3378.